

## Inclusive production of nonstrange resonances in high-energy $\nu p$ charged-current interactions

J. P. Berge, D. V. Bogert, R. J. Endorf,\* R. Hanft, J. A. Malko, and F. A. Nezzrick  
*Fermi National Accelerator Laboratory, Batavia, Illinois 60510*

G. R. Lynch, J. P. Marriner,† and M. L. Stevenson  
*Lawrence Berkeley Laboratory, University of California, Berkeley, California 94720*

R. J. Cence, F. A. Harris, M. Jones, M. W. Peters, V. Z. Peterson, V. J. Stenger, and N. Wyatt‡  
*University of Hawaii at Manoa, Honolulu, Hawaii 96822*

J. Bell, C. T. Coffin, R. N. Diamond,§ W. C. Louis,|| B. P. Roe, R. T. Ross,\*\* A. A. Seidl, and E. Wang  
*University of Michigan, Ann Arbor, Michigan 48109*

(Received 13 December 1979)

We have examined the inclusive production of nonstrange particle resonances in  $\nu p$  interactions using the Fermilab 15-ft bubble chamber. A sample of 2437 charged-current events with visible longitudinal momentum greater than 10 GeV/c was obtained. The  $\rho^0$  and  $\Delta^{++}(1232)$  are seen. An overall rate of  $0.21 \pm 0.04 \rho^0$  per event is found. For five-prong events, the rate is  $0.44 \pm 0.08 \rho^0$  per event. The  $\rho^0 Z$  distribution falls rapidly for  $Z$  greater than 0.4. The production of  $\Delta^{++}$  is seen clearly in events with an identified proton. No evidence is seen for  $\Delta^0$  production. An upper limit of 0.34 is placed on the ratio of  $\eta/\pi^0$  (90% confidence level).

### I. INTRODUCTION

The quark-parton-model view of high-energy charged-current  $\nu p$  interactions is that the intermediate  $W^+$  boson interacts with a single quark in the target nucleon and changes that quark into a quark of a different flavor. This quark then "fragments" into observed hadrons in a manner that must be determined experimentally.<sup>1</sup> The most common process in charged-current  $\nu p$  interactions is that the  $W^+$  strikes a valence  $d$  quark and changes it to a  $u$  quark. Therefore, studying details of the final-state hadron system should provide information mainly on the fragmentation of the  $u$  quark. The  $u$  quark can, in principle, fragment into resonances as well as pions and kaons. This can have important consequences for the interpretation of some of the properties (especially transverse momenta) of the observed hadrons and thus should be taken into account.<sup>2</sup> In fact, detailed studies of high-energy hadronic interactions show that a large fraction of the charged pions observed come from decays of meson and baryon resonances.<sup>3</sup> There is some additional interest in determining the rate of  $\rho^0$  production because it allows one to estimate contributions to neutrino-induced tripleton events via the decays  $\rho^0 \rightarrow \mu^-\mu^+$  or  $\rho^0 \rightarrow e^-e^+$ .

The purpose of this paper is to examine the evidence for inclusive, nonstrange-resonance production in our sample of 2437 charged-current  $\nu p$  interactions. Other details of the hadronic final state,<sup>4</sup> a study of diffractive production of

vector mesons in exclusive final states,<sup>5</sup> and a study of neutral-strange-particle production<sup>6</sup> have already been reported. In Sec. II we discuss the experimental details of event selection. Section III deals with meson-resonance production (mainly in the  $\pi^+\pi^-$  channel). In Sec. IV we discuss baryon-resonance production. In Sec. V we discuss limits on  $\eta$  production. The major conclusions are summarized in Sec. VI.

### II. EVENT SELECTION

The data come from two separate exposures of the Fermilab 15-ft hydrogen-filled bubble chamber to high-energy neutrino beams. The first (second) exposure of 70 000 (80 000) pictures was made with a wide-band, one-horn (two-horn) focused beam with  $0.52 \times 10^{18}$  ( $0.60 \times 10^{18}$ ) protons at 300 (400) GeV on target. Adding the two exposures results in a smoothly varying neutrino energy spectrum which peaks at  $\sim 15$  GeV and decreases quickly thereafter ( $\sim 90\%$  of the flux is below 100 GeV).

The film was scanned for all neutral-induced interactions. After measuring and processing through geometrical-reconstruction programs, the events were reexamined on the scan table. Events found to originate from interactions in the chamber wall or from other upstream events were removed from the sample.

The charged-current events are obtained by requiring that there be three or more prongs at the primary vertex, that the sum of the visible momenta along the incoming neutrino direction

( $\sum P_x$ ) be greater than 10 GeV/c, and that there be a selected muon. The muons are selected by a Monte Carlo-tested algorithm<sup>7</sup> which basically identifies the  $\mu^-$  candidate as being the negative track with the highest transverse momentum relative to the neutrino direction. If the track thus selected is found to interact, the event is rejected as a charged-current event. The  $\Phi_{\text{VIS}}$  and  $R_{xyz}$  cuts described in Ref. 4 are applied to reduce backgrounds from neutral-current and  $\bar{\nu}$  charged-current events. The cut on the muon transverse momentum  $P_{\text{TR}}$  is not used in this analysis for two reasons. One is that the sample is sufficiently pure without this cut; the other is to avoid potential biases against events with small values of  $x$  ( $x = Q^2/2M\nu$ ), which were not used in the analysis of Ref. 4. The above selection results in a  $\nu$  charged-current sample of 2437 events containing 7% contamination from neutral-current and  $\bar{\nu}$  charged-current events. We estimate that 17% of the  $\nu$  charged-current events are lost due to the muon selection algorithm and associated cuts. We have checked that this loss does not produce significant biases in resonance production by verifying that essentially the same results are obtained from a sample selected without the  $\Phi_{\text{VIS}}$  and  $R_{xyz}$  cuts. The incident  $K_L^0$  background is determined by using fits to the  $K_L^0 p - K_S^0 p \pi^+ \pi^-$  channel and is found to be 0.5% of the charged-current sample for  $\sum P_x > 10$  GeV/c.

The energy of the incident neutrino,  $E_\nu$ , is estimated by using a modification of a method

due to Grant. This modification is described in detail in Ref. 4. The results presented in this paper are not significantly sensitive to the particular energy estimation method employed.

### III. MESON-RESONANCE PRODUCTION

The overall  $\pi^+ \pi^-$  mass distribution is shown in Fig. 1. Only a shoulder is seen in the  $\rho^0$  region; but, because of the large combinatorial background, substantial  $\rho^0$  production may still be present. In order to examine this, a background subtraction for each multiplicity separately is made using the sum of the  $\pi^+ \pi^+$  and  $\pi^- \pi^-$  distributions as the shape of the nonresonant background in the  $\pi^+ \pi^-$  distribution. The doubly charged combinations are normalized to the  $\pi^+ \pi^-$  distribution for  $M_{\pi\pi} > 1.1$  GeV/c<sup>2</sup> to estimate the amount of nonresonant background. Unidentified protons present problems in approximating the shape of the nonresonant  $\pi^+ \pi^-$  distribution, but they are accounted for to some extent since they contribute to the  $\pi^+ \pi^+$  as well as the  $\pi^+ \pi^-$  distributions. The subtraction is done for each multiplicity separately so that the background distributions sample different regions of total hadronic mass  $W$  in the same proportion as the  $\pi^+ \pi^-$  distributions. Note that this procedure excludes 3-prong events because they do not contribute to the signal. Combining the subtracted distributions gives the lower histogram in Fig. 1. A possible enhancement in the  $\rho^0$  region and

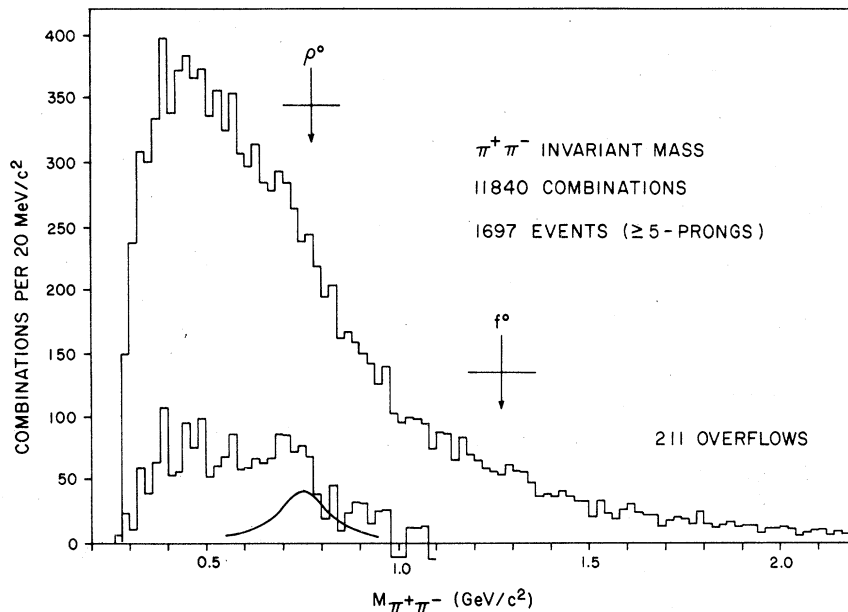


FIG. 1.  $\pi^+ \pi^-$  mass distributions for all charged-current events with  $\geq 5$  prongs. The  $\rho^0$  and  $f^0$  masses and widths are indicated at the PDG (Ref. 8) values. The lower histogram is the result after the background subtraction described in the text. The curve is a simple Breit-Wigner form normalized to the estimated  $\rho^0$  signal.

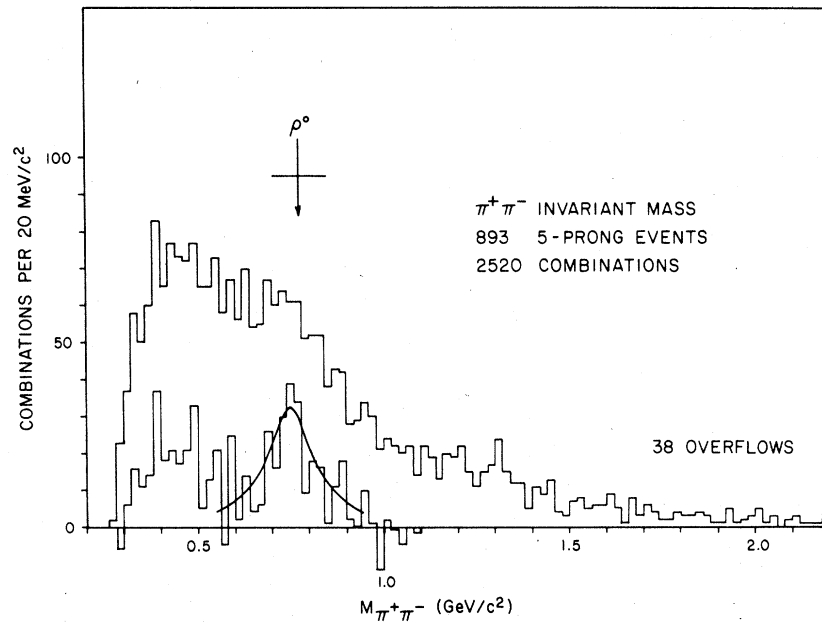


FIG. 2.  $\pi^+\pi^-$  mass distributions for 5-prong events only. The curve is a simple Breit-Wigner form normalized to the estimated  $\rho^0$  signal.

a low-mass accumulation are seen.

The  $\pi^+\pi^-$  distributions are also shown separately for 5-prong (Fig. 2), 7-prong (Fig. 3), and  $\geq 9$ -prong events (Fig. 4). A clear  $\rho^0$  signal is seen in 5-prong events but not in 7-prong or  $\geq 9$ -prong events. Therefore, we attempt to determine the rates of  $\rho^0$  production only in the overall and 5-prong event samples. The number of  $\rho^0$  is esti-

mated by taking the number of combinations above background in the range 0.7–0.8  $\text{GeV}/c^2$  and correcting for the  $\rho^0$ 's in the tails of this region using a simple energy-independent Breit-Wigner curve. The non- $\rho^0$  contribution in the 0.7–0.8  $\text{GeV}/c^2$  region is assumed to be negligible in the background-subtracted distribution for 5-prong events but that in the overall sample is estimated

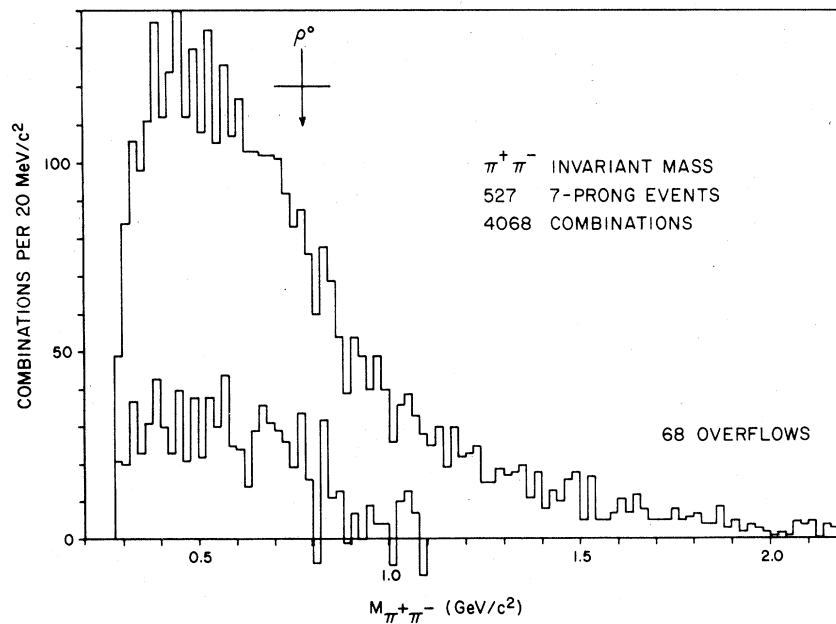
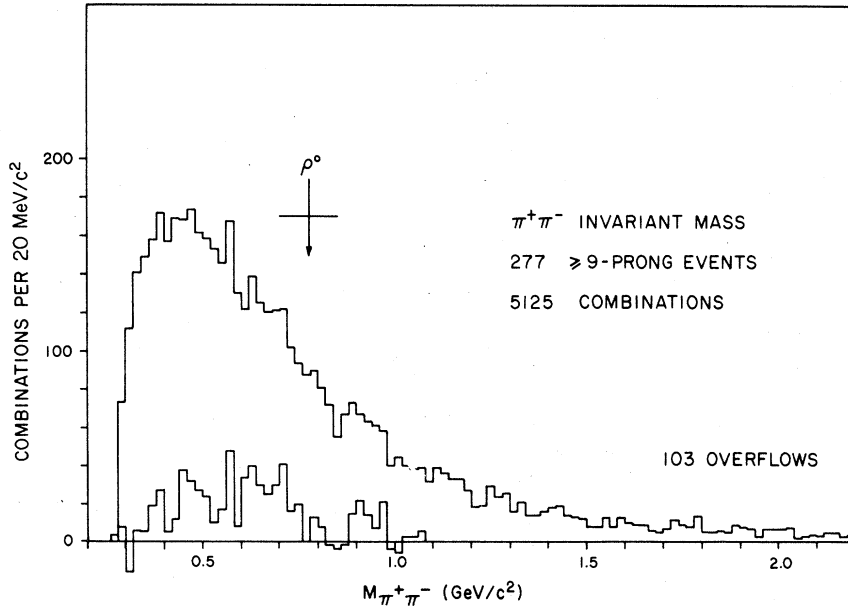


FIG. 3.  $\pi^+\pi^-$  mass distributions for 7-prong events only.

FIG. 4.  $\pi^+\pi^-$  mass distributions for  $\geq 9$ -prong events only.

by assuming a smoothly falling contribution from the low mass accumulation. The  $\rho^0$  mass  $M$  is taken to be  $0.75 \text{ GeV}/c^2$  (as indicated in the 5-prong events); the  $\rho^0$  width  $\Gamma$  is taken as the Particle Data Group<sup>8</sup> (PDG) value of  $0.155 \text{ GeV}/c^2$ . For a simple Breit-Wigner curve, the fraction  $F$  of  $\rho^0$ 's between  $E_1$  and  $E_2$ , where  $E_1 < M < E_2$ , is given by

$$F = \frac{1}{\pi} \left( \tan^{-1} \frac{E_2 - M}{\Gamma/2} + \tan^{-1} \frac{M - E_1}{\Gamma/2} \right).$$

The total number of  $\rho^0$ 's is, therefore, obtained by dividing the signal in the range  $0.7-0.8 \text{ GeV}/c^2$  by the value of  $F$  calculated using  $E_1 = 0.7$  and  $E_2 = 0.8 \text{ GeV}/c^2$ . The results are that the numbers of  $\rho^0$ 's are 510 for the overall sample and 390 for 5-prong events. For events where the hadronic invariant mass  $W$  is greater than 4 GeV, these numbers are 230 and 154 for the over-

all and 5-prong samples, respectively. The rates (i. e.,  $\rho^0$  per event) are given in Tables I and II. The errors on the rates include some estimate of the systematic uncertainty in non- $\rho^0$  contributions in the  $0.7-0.8 \text{ GeV}/c^2$  region. This uncertainty is considerably greater in the overall sample than in the 5-prong event sample. Therefore, it is significant that the clear signal in the 5-prong event sample accounts for about  $\frac{3}{4}$  of that in the overall sample. However, the fact that our  $\rho^0$  enhancement peaks below the PDG (Ref. 8) value for the  $\rho^0$  mass may indicate that the non- $\rho^0$  contributions in this mass range are not completely understood. The errors quoted on the  $\rho^0$  rates do not include an estimate of the systematic uncertainty in the nonresonant background. We have checked that changing the amount of background by normalizing the  $\pi^+\pi^-$  and doubly charged mass distributions farther out

TABLE I.  $Z$  distribution of  $\rho^0$ 's produced in charged-current events for all and high ( $W > 4 \text{ GeV}$ ) values of total hadronic mass.

$Z$ range	$\frac{1}{N_{\text{ev}}} \frac{dN}{dZ}$	
	All 2437 events	$W > 4 \text{ GeV}$ 1380 events
0-1	$0.21 \pm 0.04$	$0.17 \pm 0.03$
0-0.2	$0.28 \pm 0.12$	$0.31 \pm 0.13$
0.2-0.4	$0.46 \pm 0.12$	$0.34 \pm 0.08$
0.4-0.6	$0.23 \pm 0.07$	$0.13 \pm 0.07$
0.6-1	$0.02 \pm 0.03$	$0 \pm 0.02$

TABLE II.  $Z$  distribution of  $\rho^0$ 's produced in 5-prong events for all and high ( $W > 4 \text{ GeV}$ ) values of total hadronic mass.

$Z$ range	$\frac{1}{N_{\text{ev}}} \frac{dN}{dZ}$	
	All 893 events	$W > 4 \text{ GeV}$ 550 events
0-1	$0.44 \pm 0.08$	$0.28 \pm 0.07$
0-0.2	$0.46 \pm 0.18$	$0.49 \pm 0.22$
0.2-0.4	$0.76 \pm 0.22$	$0.52 \pm 0.18$
0.4-0.6	$0.90 \pm 0.29$	$0.44 \pm 0.22$
0.6-1	$0.033 \pm 0.034$	$0 \pm 0.03$

on the high-mass tail changes the  $\rho^0$  rates by less than quoted errors. The systematic uncertainty in the shape of the nonresonant background is harder to estimate, but the agreement in shape of the  $\pi^+\pi^-$  and doubly charged distributions above 1.1 GeV/c<sup>2</sup> gives one some confidence that this systematic uncertainty is small compared to the statistical uncertainties.

Although our limited statistics and range of total hadron invariant masses preclude quantitative comparisons with experiments studying resonance production in hadronic interactions, it seems reasonable to try to compare qualitatively. In order to have hadronic systems of the same net charge and similar total invariant masses, we compare to a detailed study<sup>9,10</sup> of  $\pi^+p$  interactions at 15 GeV/c. Our rate of 0.21  $\rho^0$ /event agrees precisely with the value obtained using the inclusive  $\rho^0$  and total cross sections of 5.07 mb (Ref. 9) and 24.05 mb (Ref. 10), respectively. Over 80% of the inclusive  $\rho^0$  production in these  $\pi^+p$  interactions is in events with 4 and 6 charged hadrons (which correspond to our 5-prong and 7-prong events). Our data show that 5-prong events contribute about  $\frac{3}{4}$  of the  $\rho^0$ 's found in the overall sample, that there is an indication of a  $\rho^0$  enhancement in 7-prong events, and that there is little  $\rho^0$  production in  $\geq 9$ -prong events. Therefore, there is qualitative agreement that most  $\rho^0$  production occurs in events with 4 or 6 charged hadrons. One interesting disagreement is that the exclusive process  $\pi^+p \rightarrow \pi^+\pi^+\pi^-p$  accounts for 14% of the total inclusive  $\rho^0$  production in these purely hadronic processes, but the exclusive process  $\nu p \rightarrow \mu^-\pi^+\pi^-\pi^+p$  (Ref. 5) accounts for only 3% of inclusive  $\rho^0$  production in our data.

The  $\rho^0$   $Z$  distributions ( $Z$  is the  $\rho^0$  momentum divided by the momentum of the total hadron system) for the overall and 5-prong event samples are presented in Tables I and II and shown in Fig. 5. The number of  $\rho^0$  giving a  $\pi^+$  or  $\pi^-$  with  $Z_r > 0.4$  is  $0.019 \pm 0.011$ /event. The distributions are of interest for comparison to the  $u$ -quark fragmentation functions into pseudoscalar mesons and are predicted by some models<sup>2</sup> that parameterize the properties of quark jets. However, the fact that the  $\rho^0$   $Z$  distributions are consistent with those for doubly charged  $\pi\pi$  combinations in the  $\rho$  mass region indicates that kinematic effects are at least as important as dynamical ones. Finally, we note that both the overall rate and  $Z$  distribution of  $\rho^0$ 's agree well with those observed in  $\bar{\nu}p$  charged-current interactions.<sup>11</sup>

Other than the  $\rho^0$ , no clear resonance signals are seen in the  $\pi^+\pi^-$  distributions. The low-mass accumulation could indicate  $\omega$  production but could also be due to isospin-zero  $\pi\pi$  scattering as seen in the exclusive process  $\bar{p}p \rightarrow 3\pi^+3\pi^-$ ,<sup>12</sup> where  $\omega$

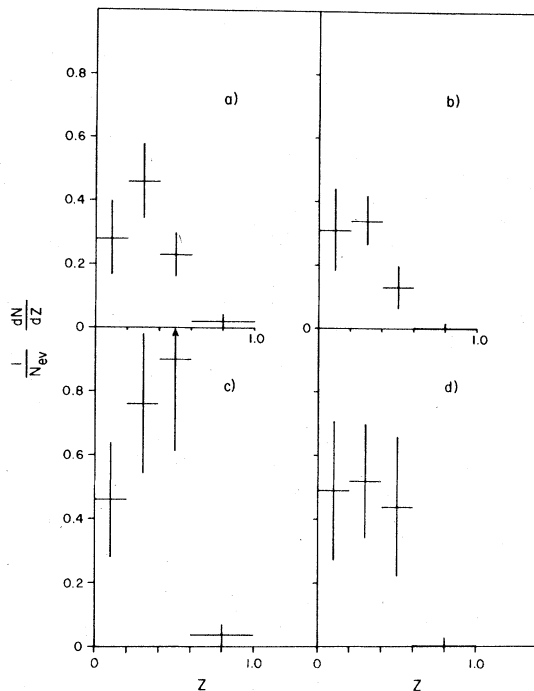


FIG. 5.  $Z$  distributions for  $\rho^0$  production in charged-current events.  $Z$  is the  $\rho^0$  momentum divided by the momentum of the total hadron system. (a) All events with  $\geq 5$  prongs. (b) All events with  $\geq 5$  prongs and total hadronic mass  $W > 4$  GeV/c<sup>2</sup>. (c) 5-prong events only. (d) 5-prong events only with  $W > 4$  GeV/c<sup>2</sup>.

production cannot be the explanation. No significant signal is seen in the region of the  $f^0$  meson. The rate of  $f^0$  production is estimated by taking the number of combinations above background (estimated from the regions above and below the  $f^0$  region) in the  $f^0$  region and by correcting for the  $f^0$ 's in the tails as done for the  $\rho^0$ 's. A simple, energy-independent Breit-Wigner form with  $f^0$  mass and width values from PDG (Ref. 8) are used. Using the mass interval 1.2–1.3 (1.1–1.4) GeV/c<sup>2</sup> as the  $f^0$  region gives a rate of  $-0.10 \pm 0.03$  ( $0.02 \pm 0.03$ )  $f^0$ /event.

The  $\pi\pi\pi$  mass distributions (not shown) have also been examined for indications of resonance production. No clear signals are seen; but, because of large combinatorial backgrounds, broad resonances could be present.

#### IV. BARYON-RESONANCE PRODUCTION

The study of baryon-resonance production is hampered by the difficulty in identifying neutrons and protons in the bubble chamber. For this study, we consider only events with an identified proton. Without this restriction, the invariant-mass distributions (not shown) are extremely difficult to interpret. Of the 2437 charged-current

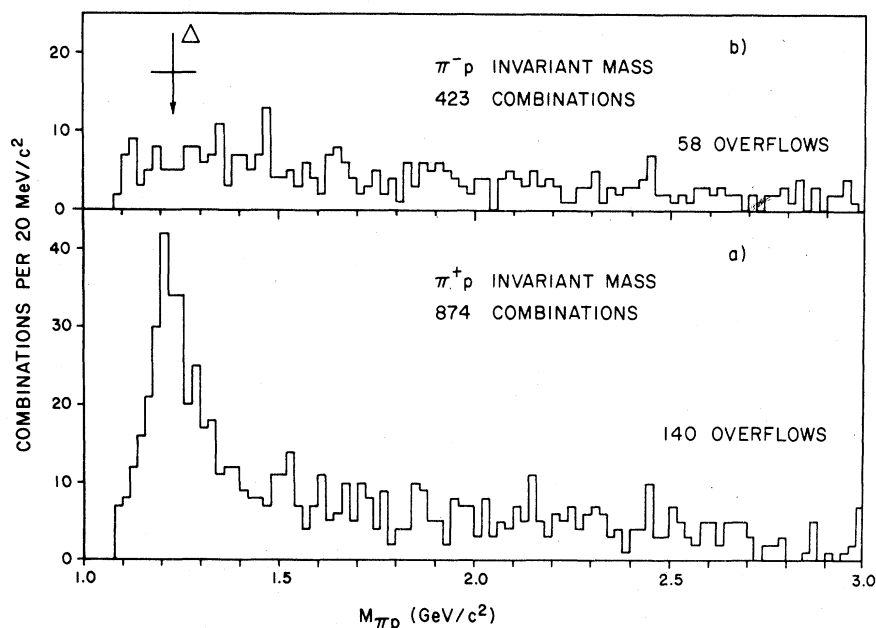


FIG. 6.  $\pi p$  mass distributions for charged-current events with identified protons. The  $\Delta$  mass and width are indicated at the PDG (Ref. 8) values. (a)  $\pi^+ p$  mass combinations. (b)  $\pi^- p$  mass combinations.

events, 455 have an identified proton. The proton is identified by range-momentum relation if it stops, or by comparison of the geometry fits using a proton versus a pion mass hypothesis if it does not stop. The algorithm used was checked using the events fitting the three-constraint (3C) reaction  $\nu p \rightarrow \mu^+ \pi^+ p$ . For momenta less than 0.5 GeV/c,  $79 \pm 5\%$  of the protons were identified; for momenta between 0.5 and 1.0 GeV/c,  $55 \pm 5\%$  of the protons were identified. For momenta less than 1 GeV/c, there is less than 1% contamination of pions in the proton sample. The method loses sensitivity at higher momentum, and very few tracks with momenta greater than 1 GeV/c are identified as protons.

Figures 6(a) and 6(b), respectively, show the  $\pi^+ p$  and  $\pi^- p$  mass distributions. A clear signal is seen for  $\Delta^{++}$  production. No clear signal for  $\Delta^0$

production is seen. The events in the region  $1.1 < M_{\pi p} < 1.4$  GeV/c<sup>2</sup> are used to estimate  $\Delta$  production rates. The background in this region is assumed to be flat and at the level of the combinations in the  $1.46 < M_{\pi p} < 1.64$  GeV/c<sup>2</sup> region. A 20% systematic uncertainty in this estimate is included in the errors in addition to the statistical errors. The corrected number of  $\Delta$  events in Table III is obtained by scaling the signal in the 1.1–1.4 GeV/c<sup>2</sup> region to correct for  $\Delta$ 's with  $M_{\pi p} > 1.4$  GeV/c<sup>2</sup>. The method is the same as that described in Sec. III to determine the  $\rho^0$  rate. A simple Breit-Wigner form with PDG (Ref. 8) values for the  $\Delta$  mass and width is used. The  $\Delta^{++}$  rates are given both with and without events in the exclusive, quasielastic  $\mu^- \pi^+ p$  final state because the  $\Delta^{++}$  production which dominates<sup>13</sup> this final state has no analog in high-energy  $\pi^+ p$  inter-

TABLE III. Estimates of  $\Delta$  production in events with an identified proton.

Distribution	Combinations with $1.1 < M_{\pi p} < 1.4$ GeV/c <sup>2</sup>	Estimated background	Net signal	Number of $\Delta$ 's Corrected for tail of Breit-Wigner form	$\Delta$ /event
$\pi^+ p$	312	115	$197 \pm 32$	$257 \pm 42$	$0.105 \pm 0.017$
$\pi^+ p$ (identified $\mu^- \pi^+ p$ removed)	262	93	$169 \pm 27$	$221 \pm 36$	$0.090 \pm 0.015$
$\pi^+ p$ ( $Z > 0.2$ and $\mu^- \pi^+ p$ removed)	98	51	$47 \pm 20$	$62 \pm 27$	$0.025 \pm 0.011$
$\pi^- p$	97	72	$25 \pm 20$	$33 \pm 27$	$0.013 \pm 0.011$
$\pi^- p$ ( $Z > 0.2$ )	19	23	$-4 \pm 9$	$-5 \pm 11$	$-0.002 \pm 0.004$

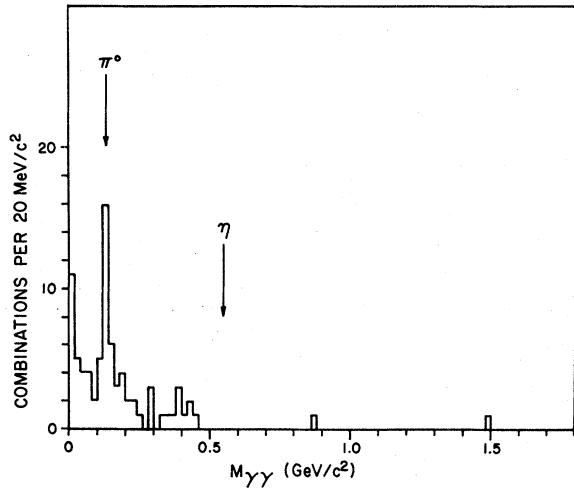


FIG. 7.  $\gamma\text{-}\gamma$  effective masses for charged-current events with more than one converted  $\gamma$  ray.

actions. Also, the description of the hadronic final state in terms of a fragmenting quark<sup>1,2</sup> is certainly inappropriate for the  $\mu^-\Delta^{**}$  final state.

The rates of  $\Delta^0$ /event in Table III are *not* corrected for events in which the proton is not identified so the true rate of  $\Delta^0$ /event may be considerably larger. Such a correction could, in principle, be done for events with protons of momenta less than 1 GeV/c by dividing the rates in Table III by the fraction of protons identified. For events with protons of momenta above 1 GeV/c, however, it is not clear how to do the correction in an unbiased way. This problem also arises in determining the ratio of  $\Delta^{**}$  to  $\Delta^0$  production where, for example, the average momentum for identified protons is significantly larger for  $\pi^-p$  combinations with  $M_{\pi^-p} < 1.4$  GeV/c<sup>2</sup> than for  $\pi^+p$  combinations in this mass range.

The  $\pi\pi p$  mass distributions (not shown) show no clear resonance signals. However, because of large combinatorial backgrounds and possible reflections of  $\rho^0$  and  $\Delta^{**}$ , broad resonances could be present.

## V. LIMITS ON $\eta$ PRODUCTION

Figure 7 shows the  $\gamma\text{-}\gamma$  mass spectrum for charged-current events with 2 or more converted  $\gamma$ 's. A clear peak is seen in the region 0.10–0.16 GeV/c<sup>2</sup> corresponding to the  $\pi^0$ . The total number of combinations in this region is 27 and the estimated background is 9 leaving  $18 \pm 6$   $\pi^0$ . Looking in the  $\eta$  region a total of zero combinations is found between 0.52 and 0.58 GeV/c<sup>2</sup>. Assuming equal detection efficiencies for  $\gamma$ 's from  $\pi^0$  and  $\eta$  decays and using the PDG (Ref. 8) branching ratio of 38% for  $\eta \rightarrow \gamma\gamma$ , a 90%-confidence-level upper limit  $\eta/\pi^0 < 0.34$  is obtained.

## VI. CONCLUSIONS

Using a sample of 2437  $\nu$ -induced charged-current events with visible longitudinal momentum greater than 10 GeV/c, we have searched for resonances in  $\gamma\gamma$ ,  $\pi\pi$ ,  $\pi\pi\pi$ ,  $\pi p$ , and  $\pi\pi p$  channels. The  $\rho^0$  is seen in the  $\pi^+\pi^-$  channel (most prominently in 5-prong events) and the  $\Delta^{**}(1232)$  is seen in the  $\pi^+p$  channel. A rate of  $0.21 \pm 0.04$   $\rho^0$  per event is found. For 5-prong events the rate is  $0.44 \pm 0.08$   $\rho^0$ /event. The  $\rho^0$   $Z$  distribution falls rapidly for  $Z$  greater than 0.4, but this may be largely a kinematic effect that is independent of the presence of the resonance.

The production of  $\Delta^{**}(1232)$  is seen clearly in events with identified protons. There are  $0.105 \pm 0.017$   $\Delta^{**}$  with an identified proton per event. No evidence is seen for  $\Delta^0$  in the  $\pi^+p$  channel. No other clear resonance signals are seen; but, because of large combinatorial backgrounds, broad resonances could be present in the  $\pi\pi\pi$  and  $\pi\pi p$  channels. Finally, a 90%-confidence-level upper limit of 0.34 is placed on the ratio of  $\eta^0$  to  $\pi^0$  production.

## ACKNOWLEDGMENT

This work is supported in part by the U. S. Department of Energy and the National Science Foundation.

\*Permanent address: University of Cincinnati, Cincinnati, Ohio 45221.

†Present address: Fermi National Accelerator Laboratory, P.O. Box 500, Batavia, Illinois 60510.

‡Present address: University College, London, England.

§Present address: Florida State University, Tallahassee, Florida 32306.

||Present address: Rutherford Laboratory, Chilton, Didcot, England.

\*\*Present address: CERN, 1211 Geneva 23, Switzerland.

<sup>1</sup>R. D. Field and R. P. Feynman, Phys. Rev. D **15**, 2590 (1977).

<sup>2</sup>R. D. Field and R. P. Feynman, Nucl. Phys. B **136**, 1 (1978).

<sup>3</sup>A recent review is given by R. Diebold, in *Proceedings of the XIX International Conference on High Energy Physics, Tokyo, 1978*, edited by S. Homma, M. Kawaguchi, and H. Miyazawa (Phys. Soc. of Japan, Tokyo, 1979), p. 666.

<sup>4</sup>J. Bell *et al.*, Phys. Rev. D **19**, 1 (1979).

<sup>5</sup>J. Bell *et al.*, Phys. Rev. Lett. **40**, 1226 (1978).

<sup>6</sup>J. P. Berge *et al.*, Phys. Rev. D **18**, 1359 (1978).

<sup>7</sup>The external muon identifier (EMI) was not used because of large accidental backgrounds in the second exposure.

See Appendix A of Ref. 4 for a description and justification of the muon-selection algorithm used here.

<sup>8</sup>Particle Data Group, Phys. Lett. 75B, 1 (1978).

<sup>9</sup>D. M. Pisello, Report No. Nevis-214, 1977 (unpublished).

<sup>10</sup>C. Baltay *et al.*, Phys. Rev. D 17, 62 (1978).

<sup>11</sup>M. Derrick *et al.*, Phys. Lett. 91B, 307 (1980).

<sup>12</sup>J. B. Gay *et al.*, Nuovo Cimento 31A, 593 (1976).

<sup>13</sup>J. Bell *et al.*, Phys. Rev. Lett. 41, 1008 (1978).